Chapter

Liquid Film Evaporation: Review and Modeling

Jamel Orfi and Amine BelHadj Mohamed

Abstract

Liquid film evaporation is encountered in various applications including in air humidifiers, in multiple effect distillers in thermal desalination, and in absorption cooling evaporators. It is associated with a falling pure, binary or multicomponent liquid film with associated complex and coupled heat and mass transfer processes. This chapter presents important fundamental aspects inherent to falling film evaporation in several geometrical configurations such as on horizontal tubes and inside inclined or vertical tubes or channels. The first part of the chapter concerns a review of recent works on this topic with emphasis on modeling and simulation features related to falling liquid films with heat and mass transfers. This document aims also to establish a frame for the modeling of the fluid flow with heat and mass transfer in the presence of evaporation. The main governing equations and the appropriate boundary and interfacial conditions corresponding to the fluid flow and associated heat and mass transfer and phase change are systematically presented and discussed for the case of falling film in a vertical channel with the presence of flowing gas mixture. Various simplifications of the governing equations and boundary and interfacial conditions have been proposed and justified. In particular, the formulation with extremely thin liquid film approximation is discussed.

Keywords: falling film, evaporation, evaporators, horizontal tubes, extremely thin films, modeling, thermal desalination, absorption

1. Introduction

Evaporation is a phase change process widely encountered in natural and industrial applications. Evaporation of a thin layer of alcohol or water in ambient air and evaporation of seawater film on a bundle of horizontal tubes of an evaporator are examples of such a complex phenomenon. Evaporation of liquid films occurs generally to ensure a cooling of the liquid itself, to cool the surface on which the liquid flows or to increase the concentration of some components in the liquid. The evaluation of the heat and mass transfer coefficients and associated evaporation rates in various configurations is an important task in the appropriate design and fabrication of multiple evaporators and heat exchangers needed in different applications including those related to microsystems. This explains why this topic has attracted an increasing and significant interest from the scientific and industrial communities. This chapter includes first, a review on the main recent works on the falling film evaporation and in a second phase, important fundamental aspects on modeling of the associated heat and mass transfer and fluid flow.

2. Literature review

In this section, updated literature survey gathering important studies on evaporation of single-component and multicomponent liquid films with associated transport phenomena and related applications will be presented and discussed. A focus will be on the modeling and simulations aspects of falling film evaporation systems.

2.1 Examples of applications of falling film evaporation

Falling film has been used in various applications. Two examples are given here. The first one concerns water desalination using falling liquid films. The second one is related to absorption refrigeration.

Multiple effect distillation (MED) is widely employed in thermal desalination industry as a mature and reliable technology. It is considered as best suited, compared to membrane-based desalination for treating feeds with high temperature and salinity [1].

Falling film evaporators are the core of the MED units. Feed preheated seawater is sprayed on the horizontal tubes as a falling film and is evaporated due to the latent heat of condensation of the steam circulating inside the tubes. The steam itself is condensing as a result of heat exchange with the evaporating feed water.

Extensive works have been published on modeling the fluid flow with heat and mass transfer in the evaporators of MED plants [2–5]. It is of interest to mention a recent work conducted by Jin et al. [5] on scale formation and crystallization modeling on horizontal tube falling evaporators used in MED. Jin et al. [5] reported the impact of various conditions of steam flow, seawater flow rate, and inlet temperature, and tube wall material and thickness on the main process performance parameters including the evaporate rate, scale growth, and overall heat transfer coefficient. The authors observed in particular that the scale layer thickness increases sharply as the feed water flow rate decreases or the tube steam temperature increases.

Another important application of falling film evaporators concerns cooling by absorption. In such systems, solution, such as LiBr-H2O, is sprayed over a bundle of horizontal tubes and a thin liquid film of solution is then formed around each tube. The percentage of the tubes surface covered by the liquid film known as "Wetting Ratio (WR)" is to be maximized for an efficient evaporation and cooling process. WR depends on various parameters including the mass flow rate per unit tube length, the solution surface tension, and the external tube surface roughness. Bu et al. [6] investigated experimentally and numerically the heat and mass transfer effectiveness of ammonia water in a falling film evaporation in vertical tube evaporators. The numerical model is based on the boundary layer equations of mass, quality, momentum, and energy for the binary ammonia-water system and solved by coordinate transformation. The experimental and numerical data are fairly compared for a various range of control parameters. The results show, in particular, that the inlet solution concentration has a strong influence on the heat transfer mechanism and the ammonia evaporation rate [6]. Papaefthimiou et al. [7] developed a two-dimensional model to investigate the heat and mass transfer inherent to water vapor absorption into an aqueous solution of LiBr. The numerical solution is obtained by solving the two-dimensional energy and species conservation equations using analytical expressions of the velocity components in x and y directions. Results on the impacts of various parameters including the liquid film Reynolds

number and the number of tubes on the total absorption rate, solution temperature, and mass flux are presented and discussed.

2.2 Overview of falling film and associated heat and mass transfer studies

There exist exhaustive studies on the falling film liquid evaporation. The particular case of falling liquid film on horizontal tubes has been extensively investigated theoretically and experimentally [8]. This case has several advantages that include its high heat transfer rate with low film flow rates, and it involves small temperature difference and has a relatively simple structure [9]. The heat transfer coefficients in falling film evaporators are very high and can vary between 700 and 4000 W/m^2K depending on the evaporating solution properties [10]. Other inherent advantages of falling film evaporation include short contact time between the fluid and the heated wall, minimal pressure drop, and minimal static head [11].

Abraham and Mani [12] proposed the thermal spray coatings to enhance the convective evaporation on horizontal tube falling film evaporators. They conducted a computational flow dynamic (CFD) analysis to predict the seawater evaporation rate and heat transfer coefficient on thermal spray-coated tubes with varying roughness under vacuum conditions. The study shows that the heat transfer coefficient increases by up to 15% due to increased roughness. However, and despite other numerous attempts to enhance the overall heat transfer process, there exist several limiting operating problems such as nonuniformity of the liquid distribution over the tubes surfaces, the presence of the non-condensable gases, and high potential of fouling and scaling mainly when dealing with salty waters.

Shear stress, gravity, and surface tension are important phenomena affecting the behavior of the falling film and the effectiveness of the evaporation process. **Figure 1** illustrates the various heat transfer processes related to liquid film falling on a horizontal cylinder.

Faghri and Zhang [13] discussed important fundamental and applied features of falling film evaporators. The basic equations giving the heat and mass transfer coefficients and the evaporation rates for various cases and configurations have been compiled and discussed. Evaporation from liquid films circulating inside channels/microchannels or horizontal/inclined walls has been described, and the related phenomena have been explained. Ribatski and Jacobi [8] developed a

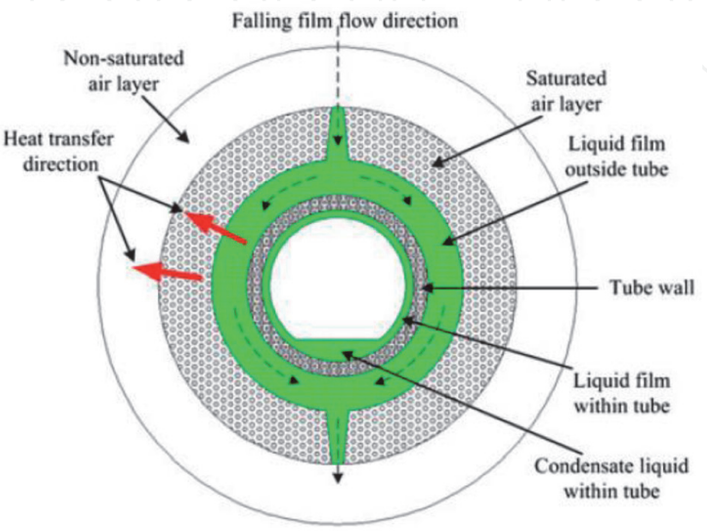

Figure 1.
Representation of heat transfer and fluid flow processes associated with falling film over a horizontal tube [9].

comprehensive and critical review on falling film evaporation on horizontal tubes. The review covers studies on heat and mass transfer performance on single tubes, finned and enhanced surfaces, and tube bundles. The authors stressed on the need to develop advanced mathematical models and accurate heat and mass transfer correlations required for the design and construction of evaporators in various applications.

The liquid film thickness and behavior are strongly linked to the heat and mass transfer coefficients and evaporation rates. It is important in the design of falling film evaporators to ensure that the film thickness is small enough to reduce the thermal resistance of the liquid layer but not too small to avoid any dry zones that may appear on the wall surface due to the rupture of the liquid which can result in various problems including fouling, corrosion, and potentially damage of the tube.

The behavior of liquid films on horizontal tubes has been investigated theoretically and experimentally in a good number of studies. It is well established that there exist three different patterns characterizing a liquid film falling over a series of horizontal tubes depending on various parameters including the liquid flow rate, the fluid properties, and the tube diameter and spacing. These flow modes are the droplet mode (the liquid leaves the tube in an intermittent way), the jet mode (the liquid leaves the tube as a continuous column), and the sheet mode (a continuous sheet is formed between the tubes) [8]. **Figure 2** describes schematically these modes.

Nusselt, as reported in [9], proposed an analytical investigation for laminar flow on horizontal tubes and one vertical or inclined wall. An expression of the film thickness by neglecting the momentum effects of the falling film was given. Similar correlation was developed by Rogers et al. [14, 15]. Later, advanced experimental methods have been used to measure the falling film thickness and characterize its patterns [10–13]. The use of these methods has led to develop clearer picture on the liquid flow structure and the associated heat and mass transfers. Besides, computational methods have been used to solve the conservation equations governing the flow and temperature fields of a falling film over surfaces [2, 14–16]. Qiu et al. [9] conducted a numerical analysis of the liquid film distribution of sheet flow on horizontal tubes. The study shows that the transient behavior of the falling film can have various stages including the free falling stage, the liquid impact stage, the liquid film developing stage, and the film fully developed stage. The presented results include the distribution of the liquid thickness with the tube diameter, the Reynolds number, and the inter-tube spacing.

Stephan [10] conducted a concise review of the heat transfer mechanisms in falling film evaporators. In particular, results and correlations on heat transfer coefficients for vertical tubes have been compiled and presented for various cases including when the falling liquid film flow is laminar, wavy laminar, and turbulent.

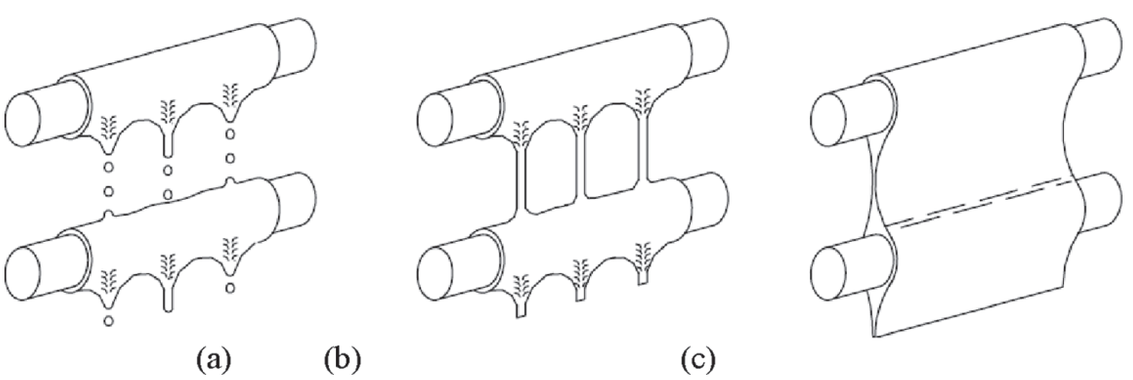

Figure 2.
The inter-tube falling film modes: (a) the droplet mode; (b) the jet mode; and (c) the sheet mode [8].

The correlations show that Nusselt number depends not only on the Reynolds and Prandtl numbers but also on Kapitza number, which measures the effect of surface tension compared to the viscous ones. Zhao et al. [17] conducted a comprehensive review on computational studies on falling liquid film flow with associated heat transfer on horizontal tubes and tube bundle. Review includes various features on falling film hydrodynamics, evaporation, and boiling outside the single tubes and the tube bundle and whole evaporator performance investigated using 2D and 3D models. Besides, previous results on falling liquid film dry-out and breakout are screened and discussed. Zhao et al. [17] concluded their review by proposing recommendations and future needs to be investigated in various fields and technologies.

There exist in general two approaches to treat numerically the heat and mass transfer associated with the evaporation of a liquid film in presence of a non-saturated gas [18–21]. The first one considers an extremely thin layer of liquid. Therefore, the governing conservation equations are simultaneously solved not only in the gas region but also in the liquid film. This requires also considering appropriate interfacial conditions between the liquid and gas phases. The second approach assumes that when the liquid film is extremely thin, the overall heat and mass transfers are not or slightly affected by the exchanges in the liquid itself. In this approach, the interfacial conditions are directly applied on the surface wall as boundary conditions. By neglecting convective terms in momentum and energy equations of the liquid, it is shown that the assumption of an extremely thin film thickness is valid only for a low mass flow rate [22]. Refs. [23–30] investigated the heat and mass transfer associated with liquid film evaporation by considering the heat transfer and fluid flow within the liquid film.

On another side, several other works have been based on the assumption of the extremely thin thickness. Cherif and Daif [21] considered the evaporation of a binary liquid film by mixed convection falling on one side of a parallel plate channel. The wetted plate is subjected to a constant and uniform heat flux, while the second one is taken as adiabatic. The authors studied the impact of using the very thin film assumption on the heat and mass transfer results. They showed in particular that the overestimation induced by considering an extremely thin film is greater for the ethylene/glycol-water mixture than for the ethanol-water mixture.

Recently, Alami et al. [31] studied the evaporative heat and mass transfer of a turbulent falling liquid film in a finite vertical tube that is partially heated. Using an implicit finite difference model, the authors solved the governing mass, species, momentum, and energy equations considering appropriate boundary and interfacial conditions. The obtained data are compared to the case of the entirely heated tube wall. Belhadj Mohamed and Tlili [32] analyzed the evaporation of a seawater film by mixed convection of humid air. In another study, Belhadj Mohamed et al. [33] considered the impact of adding metal nanoparticles to the falling liquid on the effectiveness of the evaporation process. Ma et al. [34] presented a novel model to investigate the flow and evaporation of liquid film in a rocket combustion chamber with high temperature and high shear force.

In addition to the theoretical and numerical studies on falling film evaporation, the literature includes extensive experimental research activities [35–37]. Yue et al. [35] designed and conducted a series of experiments to analyze the falling film flow behavior and evaluate the associated heat transfer outside a vertical tube. New correlations on the heat transfer coefficient and falling film dry burning have been proposed. Shahzad et al. [37] considered practical features related to the design of industrial falling film evaporators. They enumerated the main advantages of these types of evaporators and reviewed the corresponding heat transfer correlations.

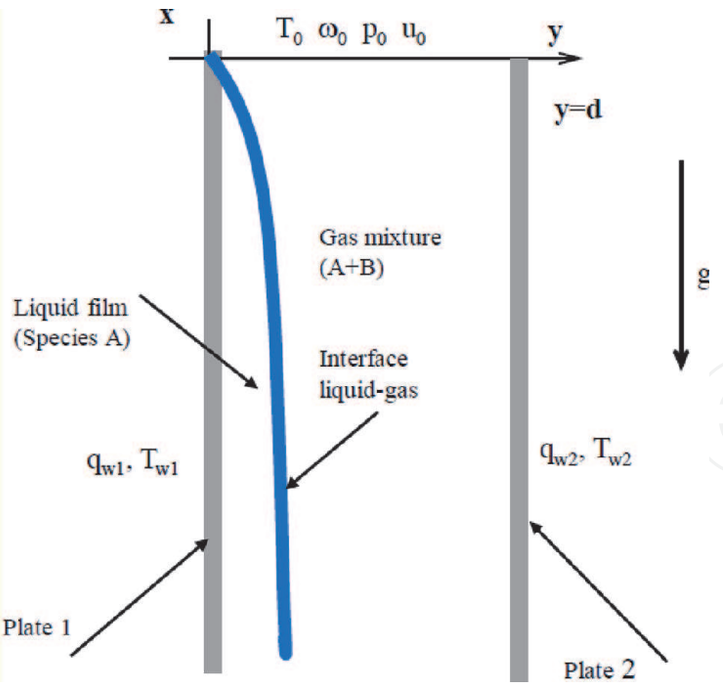

Figure 3.
Representation of the physical model.

Besides, they conducted an experimental study and proposed their own falling film heat transfer correlation.

3. Modeling of the heat and mass transfer with falling liquid film in confined channels

3.1 Introduction

We present in this section some aspects related to the theoretical formulation of the heat and mass transfer associated with liquid falling film in confined domains. We will be limited to the laminar steady state nature of flows and to the two-dimensional Cartesian configuration. We will give particular interest to the interfacial conditions equations.

3.2 Physical model description

We consider the flow of a thin liquid falling film on a plate of a vertical channel with the presence of a binary mixture gas flow. The gas and liquid flows are supposed laminar and in steady state regime. The gas mixture is composed of a non-condensable chemical species B with high concentration and a species A as vapor. This mixture can be, for example, a humid air mixture or an air-alcohol mixture. **Figure 3** shows schematically the system under study which can represent a heat and mass exchanger between a liquid film and a gas in direct contact. Various phenomena characterize this system such as thin liquid evaporation, vapor condensation, and shear stress between the gas and liquid flows. In addition, the difference in concentration that can exist between the liquid-gas interface, supposed saturated in species A as a vapor, and the neighboring gaseous mixture may result in a diffusion of the component A from the interface to the gas in case of evaporation or a reverse diffusion (from the gas toward the interface) in the condensation case.

It is worthy to mention that in absence of a forced flow of the gas mixture, the natural flow induced by the temperature and concentration gradients within the gas can be upward or downward depending on the two gases and the subjected heat and mass conditions.

3.3 Governing equations

The equations governing the flows and transfers in the two phases are those of mass, momentum, and energy equations. For laminar, steady state with no chemical reactions and neglecting the radiative heat transfer in the two fluids, the viscous dissipation and the pressure work, the conservation equations are as follows [38, 39]

3.3.1 Continuity equation

$$\frac{\partial}{\partial x}(\rho u) + \frac{\partial}{\partial y}(\rho v) = 0 \tag{1}$$

3.3.2 Momentum equations

- in x direction:

$$\rho\left(u\frac{\partial u}{\partial x} + v\frac{\partial u}{\partial y}\right) = -\frac{\partial p}{\partial x} + \frac{\partial}{\partial x}\left(2\mu\frac{\partial u}{\partial x} - \frac{2}{3}\mu\nabla\vec{V}\right) + \frac{\partial}{\partial y}\left(\mu\left(\frac{\partial u}{\partial y} + \frac{\partial v}{\partial x}\right)\right) + \rho g_x \tag{2}$$

- in y direction:

$$\rho\left(u\frac{\partial v}{\partial x} + v\frac{\partial v}{\partial y}\right) = -\frac{\partial p}{\partial y} + \frac{\partial}{\partial y}\left(2\mu\frac{\partial v}{\partial y} - \frac{2}{3}\mu\nabla\vec{V}\right) + \frac{\partial}{\partial x}\left(\mu\left(\frac{\partial u}{\partial y} + \frac{\partial v}{\partial x}\right)\right) + \rho g_y \tag{3}$$

where ρ and μ are the fluid density and dynamic viscosity, respectively; u and v are x and y components of the velocity $\vec{V}$; and p is the total pressure, while g_x and g_y are the x and y gravity acceleration components, respectively.

The total pressure can be written as the summation of the hydrostatic pressure p_0 and the dynamic pressure $(p - p_0)$. The hydrostatic pressure can be expressed as:

$$\frac{\partial p_0}{\partial x} = \rho_0 g_x = -\rho_0 g \tag{4}$$

The term $-\frac{\partial p}{\partial x} + \rho g_x$ in the Eq. (2) can be written as:

$$-\frac{\partial p}{\partial x} + \rho g_x = -\frac{\partial p}{\partial x} - \rho g = -\frac{\partial (p - p_0)}{\partial x} + (\rho_0 - \rho)g \tag{5}$$

ρ_0 is the fluid density at the reference 0. The quantity $(\rho_0 - \rho)g$ refers to natural convection generation. For small variations within the thermal and concentration fields, $(\rho_0 - \rho)$ can be expressed as function of the temperature and the concentration using the Boussinesq approximation as [39]:

In the liquid

$$(\rho_0 - \rho) = \rho_0 \beta_l (T - T_0) \tag{6}$$

β_l refers to the thermal expansion coefficient in the liquid.

In the gaseous mixture

$$(\rho_0 - \rho) = \rho_0(\beta_T(T - T_0) + \beta_w(w - w_0)) \tag{7}$$

β_T and β_w are the thermal expansion and the mass expansion coefficients, respectively. ω is the mass concentration of constituent A.

When the gas behaves as an ideal gas, β_T and β_w can be expressed respectively as:

$$\beta_T = \frac{1}{T_0} \tag{8}$$

and

$$\beta_\omega = \left(\omega_{A0} + \frac{M_A}{M_B - M_A}\right)^{-1} \tag{9}$$

M_A and M_B are the molar mass of constituent A (minority constituent) and constituent B (non-condensable majority constituent B).

For a binary ideal gas,

$$\rho = \frac{pM}{RT}, \rho_0 = \frac{p_0 M_0}{RT_0} \tag{10}$$

and (ρ-ρ_0) becomes

$$(\rho - \rho_0) = \rho\left(1 - \frac{\rho_0}{\rho}\right) = \rho\left(1 - \frac{p_0 M_0 T}{pMT_0}\right) \tag{11}$$

M stands for mixture molar mass.

The pressure variation is considered much smaller than the molar mass or temperature [39]. Then, we can have

$$\left(1 - \frac{\rho_0}{\rho}\right) \approx \left(1 - \frac{M_0}{M}\,\frac{T}{T_0}\right) \tag{12}$$

The left term in this equation can be expressed as:

$$\left(1 - \frac{\rho_0}{\rho}\right) \approx \left(1 - \frac{\rho_0}{\rho}\right)_{T=const} + \left(1 - \frac{\rho_0}{\rho}\right)_{w=const} \tag{13}$$

or:

$$\left(1 - \frac{M_0}{M}\,\frac{T}{T_0}\right) \approx \left(1 - \frac{M_0}{M}\right) + \left(1 - \frac{T}{T_0}\right) \tag{14}$$

The mixture molar mass can be expressed in terms of the molar mass of constituents A and B and their mass concentrations ω_A and ω_B as:

$$M = \frac{M_A M_B}{\omega_A M_B + \omega_B M_A} \tag{15}$$

Then:

$$\left(1 - \frac{M_0}{M}\right) \approx \left(1 - \frac{\omega_A M_B + (1 - \omega_A) M_A}{\omega_{A0} M_B + (1 - \omega_{A0}) M_A}\right) \tag{16}$$

or

$$\left(1-\frac{M_0}{M}\right)\approx\left(\frac{\omega_{A0}-\omega_A}{\omega_{A0}+\frac{M_A}{M_B-M_A}}\right) \tag{17}$$

Finally:

$$\begin{aligned}(\rho-\rho_0) &= \rho\left[\left(1-\frac{T}{T_0}\right)+\frac{\omega_{A0}-\omega_A}{\left(\omega_{A0}+\dfrac{M_A}{M_B-M_A}\right)}\right] \\ &= -\rho\left[\left(\frac{T-T_0}{T_0}\right)+(\omega_A-\omega_{A0})\left(\omega_{A0}+\frac{M_A}{M_B-M_A}\right)^{-1}\right]\end{aligned}$$

or

$$(\rho_0-\rho)=\rho[\beta_T(T-T_0)+\beta_\omega(\omega_A-\omega_{A0})] \tag{18}$$

where

$$\beta_T=\frac{1}{T_0}\text{ and }\beta_\omega=\left(\omega_{A0}+\frac{M_A}{M_B-M_A}\right)^{-1} \tag{19}$$

When one neglects ω_{A0} as compared to $\frac{M_A}{M_B-M_A}$, β_ω can be written as:

$$\beta_\omega\approx\frac{M_B-M_A}{M_A} \tag{20}$$

3.3.3 Energy conservation equation

$$\rho C_p\left(u\frac{\partial T}{\partial x}+v\frac{\partial T}{\partial y}\right)=-\frac{\partial q_x}{\partial x}-\frac{\partial q_y}{\partial y} \tag{21}$$

q_x and q_y are the x and y components of the heat flux $\vec{q}$.

3.3.4 Species conservation equation

$$\rho\left(u\frac{\partial \omega_A}{\partial x}+v\frac{\partial \omega_A}{\partial y}\right)=-\frac{\partial J_{Ax}}{\partial x}-\frac{\partial J_{Ay}}{\partial y} \tag{22}$$

J_{Ax} and J_{Ay} are the x and y mass flux components of species A with respect to average mixture velocity.

3.4 Soret and Dufour interdiffusion effects

The mass and heat fluxes $\overrightarrow{J_A}$ and $\vec{q}$, respectively, depend on the concentration and temperature gradients. They are expressed as [39–41]:

$$\vec{q}=-k\overrightarrow{grad}T+\left(\alpha_d RT\frac{M^2}{M_AM_B}+(h_A-h_B)\right)\vec{J}_A \tag{23}$$

$$\overrightarrow{J_A}=-\rho D_{AB}\left(\overrightarrow{grad}\omega_A+\alpha_d\omega_A(1-\omega_A)\overrightarrow{grad}(\ln T)\right) \tag{24}$$

α_d is a thermal diffusion factor, R is the universal gas constant, h is the specific enthalpy, k is the thermal conductivity, and D_{AB} is the coefficient of diffusion of species A in the mixture (A + B). The second and third terms of the equation giving $\vec{q}$ Eq. (23) refer to the contribution associated with the concentration gradient (Dufour effect) and with the interdiffusion of species. The second term of the equation giving the mass flux $\overrightarrow{J_A}$ Eq. (24) refers to the temperature gradient (Soret effect).

The Dufour and Soret are neglected in the majority of studies on coupled heat and mass transfers [34]. Gebhart et al. [39] reported that these effects can be neglected when the molar masses of the constituents are close and the variations in the concentration of the diffusing species are not significant. The interdiffusion of species becomes important when the difference between the specific heat coefficients of species A and B is high [41].

After substitution and adjustment, the energy and species conservation equations become

$$\rho C_p\left(u\frac{\partial T}{\partial x}+v\frac{\partial T}{\partial y}\right)=\frac{\partial}{\partial x}\left(k\frac{\partial T}{\partial x}\right)+\frac{\partial}{\partial y}\left(k\frac{\partial T}{\partial y}\right)-\frac{\partial}{\partial x}\left[\left(\frac{R}{M_AM_B}\left(\alpha_dM^2T\right)\right)+(h_A-h_B)J_{Ax}\right]-\frac{\partial}{\partial y}\left[\left(\frac{R}{M_AM_B}\left(\alpha_dM^2T\right)\right)+(h_A-h_B)J_{Ay}\right] \tag{25}$$

$$\rho\left(u\frac{\partial \omega_A}{\partial x}+v\frac{\partial \omega_A}{\partial y}\right)=\frac{\partial}{\partial x}\left(\rho D_{AB}\frac{\partial \omega_A}{\partial x}\right)+\frac{\partial}{\partial y}\left(\rho D_{AB}\frac{\partial \omega_A}{\partial y}\right)+\frac{\partial}{\partial x}\left[\rho D_{AB}\alpha_d\omega_A(1-\omega_A)\frac{1}{T}\frac{\partial T}{\partial x}\right]+\frac{\partial}{\partial y}\left[\rho D_{AB}\alpha_d\omega_A(1-\omega_A)\frac{1}{T}\frac{\partial T}{\partial y}\right] \tag{26}$$

3.5 Boundary conditions

Different types of thermal, mass, and hydrodynamic boundary conditions relating to the physical system shown schematically in **Figure** 3 can be considered. Thus and by way of illustration, we consider the situation where the two plates of the channel in **Figure** 3 are subjected to constant heat fluxes $q_{w1}$and q_{w2}. Plate 2 is impermeable and dry. This translates into:

- On plate 1 (y = 0), one can write

$$q_{w1}=q_y\Big)_{y=0}=-k_l\frac{\partial T_l}{\partial y}\Big)_{y=0} \tag{27}$$

When the liquid film thickness is negligible, one can have

$$q_{w1}=q_y\Big)_{y=0}=-k\frac{\partial T}{\partial y}\Big)_{y=0}+\left[\alpha_d\frac{RTM^2}{M_AM_B}+(h_A-h_B)\right]J_{Ay}\Big)_{y=0}+q_l \tag{28}$$

q_l refers to the latent heat transfer.

For the mass transfer, the saturation is translated by:

$$\omega)_{y=0}=\omega_{sat}(T(x,0)) \tag{29}$$

ω_{sat} stands for the saturated vapor concentration.

- Plate 2 is impermeable. The mass flux is expressed as:

$$J_{Ay}\Big)_{y=d} = -\rho D_{AB}\left[\left(\frac{\partial \omega}{\partial y} + \alpha_d \frac{\omega_A(1-\omega_A)}{T}\frac{\partial T}{\partial y}\right)\Big|_{y=d}\right] = 0 \tag{30}$$

Therefore, the diffusion mass transfer is balanced by that associated with the Soret effect.

The thermal boundary condition is reduced in this case to:

$$q_{w2} = q_y\Big)_{y=d} = -k\frac{\partial T}{\partial y}\Big)_{y=d} \tag{31}$$

- On another side, the nonslip and impermeability conditions are expressed as follows:

- On plate 1 (y = 0),

$$u_l(x, 0) = v_l(x, 0) = 0 \tag{32}$$

- On plate 2 (y = d),

$$u(x, d) = v(x, d) = 0 \tag{33}$$

It is worthy to mention that when the liquid film thickness is extremely small, the normal velocity on the plate is not zero. It can be obtained by applying a mass balance on the pas-wall interface. Let v_A, v_B and v be the local velocities of species A, B, and mixture (A + B), respectively, with respect to fixed reference. Also, $\dot{m}_A$ and $\dot{m}_B$ are the mass fluxes of A and B with respect to fixed reference.

$$\dot{m} = \dot{m}_A + \dot{m}_B \text{ or } \rho v = \rho_A v_A + \rho_B v_B \tag{34}$$

The diffusion mass flux of A, J_A is given by:

$$J_A = \rho_A(v_A - v) \tag{35}$$

then

$$\dot{m}_A = J_A + \rho_A v = J_A + \frac{\rho_A}{\rho}(\rho_A v_A + \rho_B v_B) \tag{36}$$

The interface is supposed impermeable to species B. The mass flux of B $\dot{m}_B$ is then zero on the interface. We have

$$\dot{m}_A(1-\omega_A) = J_A \Rightarrow \dot{m}_A = \rho v = \frac{J_A}{(1-\omega_A)} \tag{37}$$

Therefore

$$v = \frac{J_A}{\rho(1-\omega_A)}\Big)_{y=0} \tag{38}$$

This interfacial velocity is not known a priori because it depends on the concentration and temperature gradients at this location.

3.6 Liquid-gas interfacial conditions

3.6.1 General condition at the interface of two fluids

The fluid flow governing equations can be expressed in the following general form of a transport equation:

$$\frac{\partial \phi}{\partial t} + div\vec{f} = S \tag{39}$$

Also on an integral form:

$$\frac{d}{dt}\int_{\tau}\phi d\tau + \int_{A}\vec{f}.\vec{n}dA = \int_{\tau}Sd\tau \tag{40}$$

φ denotes the volume density of any physical quantity. $\vec{f}$ is the flux of this quantity and S is the source term. τ and A refer, respectively, to the control volume and to the control surface considered. For the continuity equation, for example, we have.

$$\phi = \rho, \vec{f} = \rho\vec{v}, \mathrm{S} = 0$$

Hsieh and Ho [42] considered a fixed control volume between two fluids (fluid 1 and fluid 2) as shown in **Figure** 4. This is a base cylinder B and height L. The height above the mobile interface is denoted by L1.

Let the mathematical function $F\left(\vec{x}, t\right)$ define the interface. $F\left(\vec{x}, t\right)$ is positive in the region of fluid 1, negative for region of fluid 2, and zero on the interface.

Applying the general Eq. (40) on the control volume of **Figure** 4:

$$\frac{d}{dt}[\phi_1 BL_1 + \phi_2 B(L - L_1)] + \left[\vec{f}_1 \cdot \frac{\overrightarrow{gradF}}{\left|\overrightarrow{gradF}\right|} - \vec{f}_2 \cdot \frac{\overrightarrow{gradF}}{\left|\overrightarrow{gradF}\right|}\right] B = SLB + o(L) \tag{41}$$

$o(L)$ refers to the flux through the lateral sides of the cylinder.

The source term can be composed of a volumetric source S_v and a surface source S_s [42, 43]:

$$\mathrm{SL} = \mathrm{S_v L} + \mathrm{S_s} \tag{42}$$

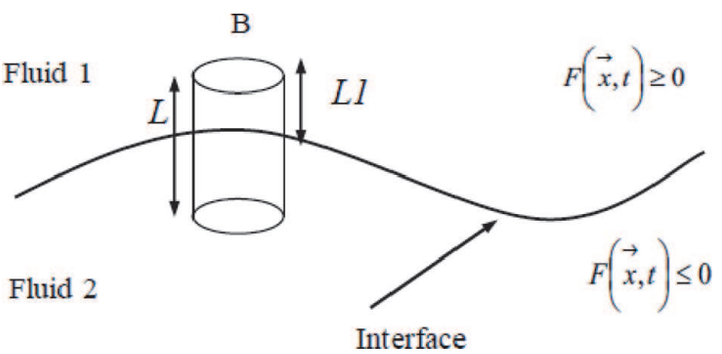

Figure 4.
Control volume at the interface between two fluids.

When L tends toward 0, Eq. (41) becomes

$$(\phi_1 - \phi_2)\frac{dL_1}{dt} + \left(\vec{f}_1 - \vec{f}_2\right)\frac{\overrightarrow{gradF}}{\left|\overrightarrow{gradF}\right|} = S_s \tag{43}$$

Consider a point M on the interface. $\vec{n}_s$ is the normal vector to the surface on M. $d\left(\overrightarrow{OM}\right)$ is the change of $\overrightarrow{OM} = \vec{x}$. The variation on $\vec{n}_s$ is $\vec{n}_s.d\left(\overrightarrow{OM}\right)$.

On the interface, $F\left(\vec{x}, t\right) = 0$. Then, one can have

$$\frac{dL_1}{dt} = -\vec{n}_s.\frac{d\vec{x}}{dt} = -\frac{\overrightarrow{gradF}}{\left|\overrightarrow{gradF}\right|}.\frac{d\vec{x}}{dt} \tag{44}$$

and

$$dF = \frac{\partial F}{\partial t}dt + \overrightarrow{gradF}.d\vec{x} = 0 \tag{45}$$

Combining Eqs. (44) and (45), one gets

$$\frac{dL_1}{dt} = \frac{\frac{\partial F}{\partial t}}{\left|\overrightarrow{gradF}\right|} \tag{46}$$

After substitution, a general condition expressing the conservation equation on the interface between the two fluids (1) and (2) can be obtained as:

$$\phi_1\frac{\partial F}{\partial t} + \vec{f}_1.\overrightarrow{gradF} = \phi_2\frac{\partial F}{\partial t} + \vec{f}_2.\overrightarrow{gradF} + S_s\left|\overrightarrow{gradF}\right| \tag{47}$$

In the following, we give some examples on how to apply this general equation to develop the mass, momentum, and energy conservation equations on the interface of two fluids. We consider the case where the fluid 1 is a binary gas mixture and the fluid 2 is a homogeneous liquid.

The function F can be chosen such as:

$$F = y - \delta \tag{48}$$

$\delta = \delta(x, t)$ is the liquid film thickness; x and y are the axial and transversal coordinates, respectively; y is measured from the wall on which the liquid flows.

Table 1 compiles the expressions of ϕ, $\vec{f}$, and S quantities associated with conservation equations of mass, momentum, energy, and species.

- The indices i and j refer to x and y coordinates, respectively.
- e stands for the internal energy and V is the magnitude of the velocity $\vec{V}$.
- σ_{ij} refers to the normal and tangential constraints. They are expressed for a Newtonian fluid [40] as:

$$\begin{cases} \sigma_{ii} = -p - \frac{2}{3}\mu.\mathrm{div}\left(\vec{V}\right) + 2\mu\frac{\partial u_i}{\partial x_i} \\ \sigma_{ij} = \mu\left(\frac{\partial u_i}{\partial x_j} + \frac{\partial u_j}{\partial x_i}\right) \\ \text{when } i \neq j \end{cases} \tag{49}$$

Conservation equation	φ	$\vec{f}$	S_s
Mass	ρ	$\rho\vec{v}$	0
Momentum	ρv_i	$f_j = \rho v_i v_j - \sigma_{ij}$	B_i
Energy	$\rho\left(e + \frac{V^2}{2}\right)$	$f_i = \rho(e + V^2/2)v_i - \sigma_{ij}v_j + q_i + g_i(\gamma)$	Q
Species	$\rho\omega_A$	$f_i = \rho\omega_A v_i + j_{Ai}$	0

Table 1.
Expressions of ϕ, $\vec{f}$, and S as function of conservation equations (compiled, adjusted and adapted from [42–44].

- B_i is the surface source term in the momentum equation. It is given by [42, 43]:

$$\vec{B} = -\vec{n}div\left(\gamma\vec{n}\right) + \overrightarrow{grad}\gamma \tag{50}$$

$\vec{n}$ is the normal vector of the interface at the point M. γ is the coefficient of surface tension. Eq. (50) shows the superposition of the tangential and normal effects of the surface tension.

- q_i and J_{Ai} represent the heat and mass fluxes on i direction.
- Q is the source term in the energy equation.
- g_i (γ) refers to the energy quantity associated with surface tension work.

3.6.2 Continuity equation case

For the conservation of mass equation, the physical quantity of interest is the mass. ϕ,$\vec{f}$ and S become ρ, $\rho\vec{v}$, and 0, respectively, as shown in **Table 1**. The interfacial general Eq. (47) becomes

$$\rho_g\left(\frac{\partial\delta}{\partial t} + u_g\frac{\partial\delta}{\partial x} - v_g\right) = \rho_l\left(\frac{\partial\delta}{\partial t} + u_l\frac{\partial\delta}{\partial x} - v_l\right) = -\xi \tag{51}$$

The indices g and l refer, respectively, to the gas and liquid.

Under steady state conditions neglecting the liquid film thickness variation, one can get

$$\rho_g v_g = \rho_l v_l \tag{52}$$

This equation states that the mass flow rate of the gas (fluid 1) leaving (arriving to) the interface is equal to the mass flow rate of the liquid (fluid 2) which arrives to (leaves) the interface.

3.6.3 Conservation of species equation case

For the case of a liquid film (fluid 2) in contact with a nonreactive gas mixture (fluid 1) composed of A (minority species) and B (noncondensable majority species), quantities ϕ and $\vec{f}$ and S are as follows:

for the liquid

$$\phi = \rho, \vec{f} = \rho\left(u\vec{i} + v\vec{j}\right) \text{ and } S = 0 \tag{53}$$

for the gas

$$\phi = \rho\omega_A, \vec{f} = (\rho\omega_A u + J_{Ax})\vec{i} + \left(\rho\omega_A v + J_{Ay}\right)\vec{j} \text{ and } S = 0 \tag{54}$$

The general equation on the liquid-gas interface becomes under these conditions:

$$\begin{aligned}&\rho_g\omega_A\left(-\frac{\partial\delta}{\partial t}\right) + \left[\left(\rho_g\omega_A u_g + j_{Ax}\right)\left(-\frac{\partial\delta}{\partial x}\right) + \left(\rho_g\omega_A v_g + J_{Ay}\right)\right] \\ &= \rho_l\left(-\frac{\partial\delta}{\partial t}\right) + \rho_l u_l\left(-\frac{\partial\delta}{\partial x}\right) + \rho_l v_l\end{aligned} \tag{55}$$

For steady state regime, one can have

$$\left[\left(\rho_g\omega_A u_g + j_{Ax}\right)\left(-\frac{\partial\delta}{\partial x}\right) + \left(\rho_g\omega_A v_g + J_{Ay}\right)\right] = \rho_l u_l\left(-\frac{\partial\delta}{\partial x}\right) + \rho_l v_l \tag{56}$$

When in addition the liquid film thickness varies very little, one can get

$$\rho_g\omega_A v_g + J_{Ay} = \rho_l v_l \tag{57}$$

Under these conditions, we have also based on Eq. (52) $\rho_g v_g = \rho_l v_l$,
or

$$v_g = \frac{J_{Ay}}{\rho_g(1 - w_A)} \tag{58}$$

J_{Ay} can be given by the Fick's law, the gas velocity on the interface is expressed as:

$$v_g = -\frac{D_{AB}}{(1 - w_A)}\frac{\partial w_A}{\partial y} \tag{59}$$

3.6.4 Momentum equation case

In this case, the variable of interest is the momentum equation in the i direction. The variables $\phi$and $\vec{f}$ can be expressed as:
In the x direction:

$$\phi = \rho u \text{ and } \vec{f} = (\rho uu - \sigma_{xx})\vec{i} + (\rho uv - \sigma_{xy})\vec{j} \tag{60}$$

In the y direction:

$$\phi = \rho v \text{ and } \vec{f} = (\rho uv - \sigma_{xy})\vec{i} + (\rho vv - \sigma_{yy})\vec{j} \tag{61}$$

σ_{xx}, σ_{yy}, and σ_{xy} are the normal and tangential constraints for a Newtonian fluid. They are expressed in Eq. (49).

The surface source term S_s, which is related to the surface tension effects, is given by Eq. (50). The surface tension coefficient γ can vary along the interface if this interface is nonhomogeneous for example. For a homogeneous interface, this coefficient can be taken as constant. Eq. (50) becomes

$$\vec{S}_s = -\overrightarrow{\gamma n}\, div\left(\vec{n}\right) \tag{62}$$

$\vec{n}$ is the normal vector to the fluid 2 surface:
Given that

$$div\left(\vec{n}\right) = div\left(\frac{\overrightarrow{gradF}}{\left|\overrightarrow{gradF}\right|}\right) = \left(\frac{1}{R1}+\frac{1}{R2}\right) \tag{63}$$

where R1 and R2 are the radii of curvature of the interface.

Therefore, the general equation at the interface (16) becomes the momentum conservation case:

in x:

$$\begin{aligned}&\rho_g u_g\left(-\frac{\partial\delta}{\partial t}\right)+\left[\left(\rho_g u_g u_g-\sigma_{xx,g}\right)\left(-\frac{\partial\delta}{\partial x}\right)+\left(\rho_g u_g v_g-\sigma_{xy,g}\right)\right]\\&=\rho_l u_l\left(-\frac{\partial\delta}{\partial t}\right)+\left[\left(\rho_l u_l u_l-\sigma_{xx,l}\right)\left(-\frac{\partial\delta}{\partial x}\right)+\left(\rho_l u_l v_l-\sigma_{xy,l}\right)\right]\\&\quad-\gamma\left(\frac{1}{R1}+\frac{1}{R2}\right)\left(-\frac{\partial\delta}{\partial x}\right)\end{aligned} \tag{64}$$

in y:

$$\begin{aligned}&\rho_g v_g\left(-\frac{\partial\delta}{\partial t}\right)+\left[\left(\rho_g u_g v_g-\sigma_{xy,g}\right)\left(-\frac{\partial\delta}{\partial x}\right)+\left(\rho_g v_g v_g-\sigma_{yy,g}\right)\right]\\&=\rho_l v_l\left(-\frac{\partial\delta}{\partial t}\right)+\left[\left(\rho_l u_l v_l-\sigma_{xy,l}\right)\left(-\frac{\partial\delta}{\partial x}\right)+\left(\rho_l v_l v_l-\sigma_{yy,l}\right)\right]\\&\quad-\gamma\left(\frac{1}{R1}+\frac{1}{R2}\right)\end{aligned} \tag{65}$$

Or after substitution and arrangement:

in x:

$$\begin{aligned}&u_g\zeta+\left[-p_g-\frac{2}{3}\mu_g\left(\frac{\partial u_g}{\partial x}+\frac{\partial v_g}{\partial y}\right)+2\mu_g\frac{\partial u_g}{\partial x}\right]\left(\frac{\partial\delta}{\partial x}\right)-\mu_g\left(\frac{\partial u_g}{\partial y}+\frac{\partial v_g}{\partial x}\right)=\\&u_l\zeta+\left[-p_l-\frac{2}{3}\mu_l\left(\frac{\partial u_l}{\partial x}+\frac{\partial v_l}{\partial y}\right)+2\mu_l\frac{\partial u_l}{\partial x}\right]\left(\frac{\partial\delta}{\partial x}\right)-\mu_l\left(\frac{\partial u_l}{\partial y}+\frac{\partial v_l}{\partial x}\right)\\&\quad+\gamma\left(\frac{1}{R1}+\frac{1}{R2}\right)\left(\frac{\partial\delta}{\partial x}\right)\end{aligned} \tag{66}$$

in y:

$$v_g\zeta + (\mu_g\left(\frac{\partial u_g}{\partial y}+\frac{\partial v_g}{\partial x}\right)\left(\frac{\partial \delta}{\partial x}\right) - \left[-p_g - \frac{2}{3}\mu_g\left(\frac{\partial u_g}{\partial x}+\frac{\partial v_g}{\partial y}\right) + 2\mu_g\frac{\partial v_g}{\partial y}\right] =$$
$$v_l\zeta + (\mu_l\left(\frac{\partial u_l}{\partial y}+\frac{\partial v_l}{\partial x}\right)\left(\frac{\partial \delta}{\partial x}\right) - \left[-p_l - \frac{2}{3}\mu_l\left(\frac{\partial u_l}{\partial x}+\frac{\partial v_l}{\partial y}\right) + 2\mu_l\frac{\partial v_l}{\partial y}\right] \quad (67)$$
$$-\gamma\left(\frac{1}{R1}+\frac{1}{R2}\right)$$

ζ is defined in Eq. (51).

Eqs. (66) and (67) express the momentum conservation on the liquid-gas interface in presence of phase change (evaporation/condensation) and surface tension. They can lead to easier expressions depending on the approximations considered.

Thus, for steady state and neglected liquid thickness, one can get in x direction:

$$\rho_g u_g v_g - \mu_g\left(\frac{\partial u_g}{\partial y}+\frac{\partial v_g}{\partial x}\right) = \rho_l u_l v_l - \mu_l\left(\frac{\partial u_l}{\partial y}+\frac{\partial v_l}{\partial x}\right) \quad (68)$$

Considering Eq. (52) and the nonslip condition between the two phases (liquid-gas) ($u_g = u_l$) Eq. (68) becomes

$$\mu_g\left(\frac{\partial u_g}{\partial y}+\frac{\partial v_g}{\partial x}\right) = \mu_l\left(\frac{\partial u_l}{\partial y}+\frac{\partial v_l}{\partial x}\right) \quad (69)$$

in y direction:

$$\rho_g v_g v_g - \left[-p_g - \frac{2}{3}\mu_g\left(\frac{\partial u_g}{\partial x}+\frac{\partial v_g}{\partial y}\right) + 2\mu_g\frac{\partial v_g}{\partial y}\right] =$$
$$\rho_l v_l v_l - \left[-p_l - \frac{2}{3}\mu_l\left(\frac{\partial u_l}{\partial x}+\frac{\partial v_l}{\partial y}\right) + 2\mu_l\frac{\partial v_l}{\partial y}\right] - \gamma\left(\frac{1}{R1}+\frac{1}{R2}\right) \quad (70)$$

We can observe that in these conditions, the surface tension effects appear just in y direction.

When the boundary layer approximations are used neglecting the surface tension effects, the following equations widely adopted in the literature are obtained:

$$\mu_g\left(\frac{\partial u_g}{\partial y}\right) = \mu_l\left(\frac{\partial u_l}{\partial y}\right) \quad (71)$$

$$p_g = p_l \quad (72)$$

3.6.5 Conservation of energy equation case

For the energy equation, the variables ϕ and $\vec{f}$ should correspond to the followings (see **Table 1**):

$$\phi = \rho\left(e + \frac{V^2}{2}\right) \quad (73)$$

$$\vec{f} = \left[\rho\left(e+\frac{V^2}{2}\right)u - \sigma_{xx}u - \sigma_{xy}v + q_x + g_x(\gamma)\right]\vec{i} + \left[\rho\left(e+\frac{V^2}{2}\right)v - \sigma_{yx}u - \sigma_{yy}v + q_y + g_y(\gamma)\right]\vec{j} \tag{74}$$

When the source term is zero and the work associated with the surface tension forces is neglected, the use of the general Eq. (47) gives

$$\left(e_g+\frac{V_{g2}}{2}\right)\zeta + \left\{\left[-p_g - \frac{2}{3}\mu_g\left(\frac{\partial u_g}{\partial x}+\frac{\partial v_g}{\partial y}\right) + 2\mu_g\frac{\partial u_g}{\partial x}\right]u_g + \left[\left(\mu_g\left(\frac{\partial u_g}{\partial y}+\frac{\partial v_g}{\partial x}\right)\right]v_g - q_{x,g}\right\}\left(\frac{\partial \delta}{\partial x}\right) - \left[\left[\left(\mu_g\left(\frac{\partial u_g}{\partial y}+\frac{\partial v_g}{\partial x}\right)\right]u_g + \left[-p_g - \frac{2}{3}\mu_g\left(\frac{\partial u_g}{\partial x}+\frac{\partial v_g}{\partial y}\right) + 2\mu_g\frac{\partial v_g}{\partial y}\right]v_g - q_{y,g}\right] =$$

$$\left(e_l+\frac{V_{l2}}{2}\right)\zeta + \left\{\left[-p_l - \frac{2}{3}\mu_l\left(\frac{\partial u_l}{\partial x}+\frac{\partial v_l}{\partial y}\right) + 2\mu_l\frac{\partial u_l}{\partial x}\right]u_l + \left[\left(\mu_l\left(\frac{\partial u_l}{\partial y}+\frac{\partial v_l}{\partial x}\right)\right]v_l - q_{x,l}\right\}\left(\frac{\partial \delta}{\partial x}\right) - \left[\left[\left(\mu_l\left(\frac{\partial u_l}{\partial y}+\frac{\partial v_l}{\partial x}\right)\right]u_l + \left[-p_l - \frac{2}{3}\mu_l\left(\frac{\partial u_l}{\partial x}+\frac{\partial v_l}{\partial y}\right) + 2\mu_l\frac{\partial v_l}{\partial y}\right]v_l - q_{y,l}\right] \tag{75}$$

If in addition, the flow is steady state and the work of the friction forces and kinetic energy terms are ignored, and Eq. (75) becomes

$$\left(e_g+\frac{p_g}{\rho_g}\right)\left[-\rho_g\left(u_g\frac{\partial \delta}{\partial x} - v_g\right)\right] + q_{y,g} - q_{x,g}\frac{\partial \delta}{\partial x} = \left(e_l+\frac{p_l}{\rho_l}\right)\left[-\rho_l\left(u_l\frac{\partial \delta}{\partial x} - v_l\right)\right] + q_{y,l} - q_{x,l}\frac{\partial \delta}{\partial x} \tag{76}$$

This equation can be further simplified by assuming a small axial variation of the liquid film thickness. Using the specific enthalpy h, one can obtain

$$h_g\rho_g v_g + q_{y,g} = h_l\rho_l v_l + q_{y,l} \tag{77}$$

Knowing in these conditions that $\rho_g v_g = \rho_l v_l$ (Eq. (52)) and assuming the interface is impermeable to the species B, one can write

$$\rho_g v_g = \rho_A v_A + \rho_B v_B = \rho_A v_A \tag{78}$$

$$\rho_g v_g h_g = \rho_A v_A h_A + \rho_B v_B h_B = \rho_A v_A h_A \tag{79}$$

or

$$h_g = h_A \tag{80}$$

Eq. (75) becomes

$$q_{y,g} + \dot{m}h_{fg} = q_{y,l} \tag{81}$$

$\dot{m}$ is the liquid evaporation rate and h_{fg} is the latent heat enthalpy.

By substituting the expressions of $q_{y,g}$ and $q_{y,l}$, one can have

$$\dot{m}h_{fg} - k_g \frac{\partial T_g}{\partial y} + \left[\alpha_d R T_g \frac{M^2}{M_A M_B} + (h_A - h_B)\right] J_{Ay,g} = -k_l \frac{\partial T_l}{\partial y} \tag{82}$$

When the Dufour and the interdiffusion of spices effects in the heat flux expression are neglected:

$$\dot{m}h_{fg} - k_g \frac{\partial T_g}{\partial y} = -k_l \frac{\partial T_l}{\partial y} \tag{83}$$

This equation is a simplified condition expressing the energy balance at the liquid-gas interface.

It is important to mention that in the majority of the theoretical works published on the coupled heat and mass transfers in the presence of falling films, numerous assumptions and approximations are retained and used which leads to simple and flexible balance equations on the interfaces.

4. Conclusion

Falling film evaporation is widely encountered in various natural and industrial applications. It encompasses multiple physical phenomena associated with surface tension, shear stress, heat and mass transfer, and others. This book chapter reviews the main studies on falling film evaporation, especially those related to numerical treatment and modeling.

Besides, a frame for the modeling of the fluid flow with heat and mass transfer in presence of evaporation has been established and explained. Therefore, we have presented various aspects related to the formulation of the coupled heat and mass transfer problem with or without falling film. A general interface balance equation was derived and subsequently used to establish the conditions expressing the conservation of energy, mass, and momentum at the interface between a falling liquid and a gas mixture inside confined domain.

Author details

Jamel Orfi[1,2*] and Amine BelHadj Mohamed[3]

1 Mechanical Engineering Department, King Saud University, Riyadh, Saudi Arabia

2 KA CARE Energy Research and Innovation Center, Riyadh, Saudi Arabia

3 Thermal and Energy Systems Studies Laboratory, National School of Engineers of Monastir, Monastir, Tunisia

*Address all correspondence to: orfij@ksu.edu.sa

References

[1] Jamil MA, Zubair SM. Effect of feed flow arrangement and number of evaporators on the performance of multi-effect mechanical vapor compression desalination systems. Desalination. 2018;**429**:76-87. DOI: 10.1016/j.desal.2017.12.007

[2] Wunder F, Enders S, Semiat R. Numerical simulation of heat transfer in a horizontal falling film evaporator of multiple-effect distillation. Desalination. 2018;**401**:206-229. DOI: 10.1016/j.desal.2016.09.020

[3] Ribatski G, Jacobi AM. Falling-film evaporation on horizontal tubes – a critical review. International Journal of Refrigeration. 2005;**28**:635-653

[4] Qiu Q, Zhu X, Mu L, Shen S. An investigation on the falling film thickness of sheet flow over a completely wetted horizontal round tube surface. Desalination and Water Treatment. 2016;**57**(35):16277-16287. DOI: 10.1080/19443994.2015.1079803

[5] Stephan K. Heat Transfer in Condensation and Boiling. Berlin Heidelberg Gmb H: Springer-Verlag; 1992

[6] Bu X, Weibin MA, Huashan LI. Heat and mass transfer of ammonia-water in falling film evaporator. Frontier in Energy. 2011;**5**(4):358-366

[7] Papaefthimiou VD, Koronaki IP, Karampinos DC, Rogdakis ED. A novel approach for modelling LiBr–H2O falling film absorption on cooled horizontal bundle of tubes. International Journal of Refrigeration. 2012;**35**(4): 1115-1122. DOI: 10.1016/j.ijrefrig.2012.01.015

[8] Raju A, Mani A. Effect of flame spray coating on falling film evaporation for multi effect distillation system. Desalination and Water Treatment. 2013;**51**(4–6):822-829

[9] Faghri A, Zhang Y. Transport Phenomena in Multiphase Systems. Amesterdam, NL: Elsevier; 2006

[10] Rogers JT. Laminar falling film flow and heat transfer characteristics on horizontal tubes. Canadian Journal of Chemical Engineering. 1981;**59**:213-222. DOI: 10.1002/cjce.5450590212

[11] Rogers JT, Goindi SS. Experimental laminar falling film heat transfer coefficients on a large diameter horizontal tube. Canadian Journal of Chemical Engineering. 1989;**67**:560-568. DOI: 10.1002/cjce.5450670406

[12] Zhang JT, Wang BX, Peng XF. Falling liquid film thickness measurement by an optical-electronic method. The Review of Scientific Instruments. 2000;**71**:1883-1886. DOI: 10.1063/1.1150557

[13] Gstoehl D, Roques JF, Crisinel P, Thome JR. Measurement of falling film thickness around a horizontal tube using a laser measurement techniquere. Heat Transfer Engineering. 2004;**25**:28-34. DOI: 10.1080/01457630490519899

[14] Wang XF, He MG, Fan HL, Zhang Y. Measurement of falling film thickness around a horizontal tube using laser-induced fluorescence technique. In: The 6th International Symposium on Measurement Techniques for Multiphase Flows. Vol. 147. 2009. pp. 1-8

[15] Hou H, Bi QC, Ma H, Wu G. Distribution characteristics of falling film thickness around a horizontal tube. Desalination. 2012;**285**:393-398. DOI: 10.1016/j.desal.2011.10.020

[16] Bigham S, Kouhi Kamali R, Noori SMA, Abadi R. Two-phase flow numerical simulation and experimental verification of falling film evaporation

on a horizontal tube bundle. Desalination and Water Treatment. 2015;**55**:2009-2022. DOI: 10.1080/19443994.2014.937750

[17] Zhao CY, Qi D, Ji WT, Jin PH, Tao WQ. A comprehensive review on computational studies of falling film hydrodynamics and heat transfer on the horizontal tube and tube bundle. Applied Thermal Engineering. 2022; **202**:117869. DOI: 10.1016/j.applthermaleng.2021.117869

[18] Bu X, Ma W, Huang Y. Numerical study of heat and mass transfer of ammonia-water in falling film evaporator. Heat and Mass Transfer. 2012;**48**:725-734. DOI: 10.1007/s00231-011-0923-4

[19] Boukrani K, Carlier C, Gonzalez A, Suzanne P. Analysis of heat and mass transfer in asymmetric system. International Journal of Thermal Sciences. 2000;**39**:130-139. DOI: 10.1016/S1290-0729(00)001987

[20] Yan WM. Effects of film evaporation on laminar mixed heat and mass transfer in a vertical channel. International Journal of Heat and Mass Transfer. 1992;**35**(12):3419-3429

[21] Ali Cherif A, Daif A. Etude numérique du transfert de chaleur et de masse entre deux plaque planes verticales en présence d'un film de liquide binaire ruisselant sur l'une des plaques chauffées. International Journal of Heat and Mass Transfer. 1999;**42**(13): 2399-2418. DOI: 10.1016/S0017-9310(98)00339-1

[22] Yan WM, Lin TF. Evaporative cooling of liquid film through interfacial heat and mass transfer in a vertical channel: Numerical study. International Journal of Heat and Mass Transfer. 1991; **34**:1124-1191

[23] Feddaoui M, Belahmidi E, Mir BA. Numerical study of the evaporative cooling liquid film in laminar mixed convection tube flows. International Journal of Thermal Science. 2001;**40**: 1011-1020

[24] Agunaoun A, Daif A, Barriol R, Daguenet M. Evaporation en convection forcée d'un film mince s'écoulant en régime permanent, laminaire et sans ondes sur une surface plane inclinée. International Journal of Heat and Mass Transfer. 1994;**37**:2947-2956

[25] Agunaoun A, Ilidrissi A, Daif A, Barriol R. Etude de l'évaporation en convection mixte d'un film liquide d'un mélange binaire s'écoulant sur un plan incliné soumis à un flux de chaleur constant. International Journal of Heat and Mass Transfer. 1998;**41**(14): 2197-2210

[26] Mezaache E, Dagunet M. Etude numérique de l'évaporation dans un courant d'air laminaire d'un film d'eau ruisselant sur une plaque inclinée. International Journal of Thermal Science. 2000;**39**:117-129

[27] Feddaoui M, Mir A, Belahmidi E. Numerical simulation of mixed convection heat and mass transfer with liquid film cooling along an insulated vertical channel. Heat and Mass Transfer. 2003;**39**:445-453. DOI: 10.1007/s00231-002-0340-9

[28] Tahir F, Mabrouk A, Koç M. Heat transfer coefficient estimation of falling film for horizontal tube multi-effect desalination evaporator using CFD. International Journal of Thermofluids. 2021;**11**:100101

[29] Abraham R, Mani A. Heat transfer characteristics in horizontal tube bundles for falling film evaporation in multi-effect desalination system. Desalination. 2015;**375**:129-137. DOI: 10.1016/j.desal.2015.06.018

[30] Jin PH, Zhang Z, Mostafa I, Zhao CY, Ji WT, Tao WQ. Heat transfer

correlations of refrigerant falling film evaporation on a single horizontal smooth tube. International Journal of Heat and Mass Transfer. 2019;**133**: 96-106. DOI: 10.1016/j.applthermaleng.2016.02.090

[31] Alami S, Feddaoui M, Nait Alla A, Bammou L, Souhar K. Turbulent liquid film evaporation in a partially heated wall along a vertical tube. Heat Transfer. 2021;**50**(3):2220-2241. DOI: 10.1002/htj.21975

[32] Belhadj Mohamed A, Tlili I. Evaporation of a saltwater film in a vertical channel and comparison with the case of the freshwater. Journal of Energy Resources Technology. 2020; **142**(11):103-112. DOI: 10.1115/1.4047250

[33] Belhadj Mohamed A, Hdidi W, Tlili I. Evaporation of water/alumina nanofluid film by mixed convection inside heated vertical channel. Applied Sciences. 2020;**10**(7):2380

[34] Ma X, Wang Y, Tian W. A novel model of liquid film flow and evaporation for thermal protection to a chamber with high temperature and high shear force. International Journal of Thermal Sciences. 2022;**172**:107300

[35] Yue Y, Yang J, Li X, Song Y, Zhang Y, Zhang Z. Experimental research on falling film flow and heat transfer characteristics outside the vertical tube. Applied Thermal Engineering. 2021;**199**:117592. DOI: 10.1016/j.applthermaleng.2021.117592

[36] Zhang Z, Wang X, Chen Q, Zhang T. Experimental study on enhanced heat transfer tubes in falling film evaporation. Journal of Physics: Conference Series. 2021;**2021**(2029): 012042

[37] Shahzad MW, Burhan M, Ng KC. Design of industrial falling film evaporators. In: Iranzo A, editor. Heat and Mass Transfer: Advances in Science and Technology Applications. London: InTech Open; 2019

[38] Mahajan RL, Wei C. Buyancy, Soret, Dufour variable property effects in Silicon Epitaxy. Journal of Heat Transfer-Transactions of the ASME. 1991;**113**:688

[39] Gebhart B, Jaluria Y, Mahajan R L, Sammakia B. Buoyancy-induced Flows and Transport. Washington DC, USA: 1988

[40] Bird RB, Stewart WE, Lightfoot EN. Transport Phenomena. New York, USA: Wiley; 2007

[41] Weaver JA, Viskanta R. Natural convection in binary gases driven by combined horizontal thermal and vertical solute gradients. Experimental Thermal and Fluid Science. 1992;**59**(1): 57-68

[42] Hsieh DY, Ho SP. Wave and Stability in Fluids. Singapore: World Scientific Pub Co Inc; 1994

[43] Bel Hadj Mohamed A. Etude du ruissellement d'un film en présence de changement de phase, Msc thesis Report, National School of Engineering of Monastir, 2001

[44] Orfi J. Heat and mass transfer with phase change between a falling liquid film and a flowing gas, 'Transferts de chaleur et de masse avec changement de phase entre un film liquide tombant et un gaz en écoulement' (in French), Post-doctoral degree report, Rapport d'Habilitation de Recherche HDR, Faculty of Sciences of Tunis, University of Tunis-AlManar. 2006